Journal of Power Sources 266 (2014) 7–21

Contents lists available at ScienceDirect

Journal of Power Sources

journal homepage: www.elsevier.com/locate/jpowsour

Optimum design of a fuel-cell powertrain based on multiple design criteria

Ismail Levent Sarioglu [a,b,*], Bartosch Czapnik [a], Emine Bostanci [a], Olaf P. Klein [a], Hendrik Schröder [a], Ferit Küçükay [b]

[a] Group Research Powertrain Systems, Volkswagen AG, Letterbox 011/17780, Wolfsburg 38436, Germany
[b] Institute of Automotive Engineering, Technical University of Braunschweig, Hans-Sommer-Straße 4, 38106 Braunschweig, Germany

HIGHLIGHTS

- Numerous customer-related design objectives are considered in optimization.
- Combining the simulation results with analytical methods increases the accuracy.
- Computing the entire search space provides valuable data for the trade-off analysis.
- Influences of individual design choices on a customer profile are analyzed.
- Favorable design options are presented by varying the weightings of design objectives.

ARTICLE INFO

Article history:
Received 14 November 2013
Received in revised form
18 March 2014
Accepted 11 April 2014
Available online 14 May 2014

Keywords:
Fuel cell
Powertrain
Design
Hybrid
Multiobjective
Optimization

ABSTRACT

As the number of fuel-cell vehicles on the roads increase, the vehicle designs are gaining more importance. Clearly, one major topic in this field is the optimization of powertrain designs. In this design process, the aim of the car manufacturers is to meet the expectations of the potential customer best, while creating a sustainable product. However, due to several trade-offs in the design, it would be non-realistic to expect a single solution that fulfills all design objectives. Therefore, a systematical approach, which includes a trade-off analysis and evaluation methods for this multiobjective design problem, is required. In this paper, a suitable methodology is presented and applied in a case study, where an optimum powertrain design for a typical European long-range passenger car is sought. Simulation-aided powertrain models and scalable component models are used to increase the accuracy of the design process. Furthermore, various visual and quantitative evaluation techniques are applied in order to support the decision making process.

1. Introduction

Fuel cell vehicles (FCVs) represent an important concept to meet the future challenges, like the reduction of fossil fuel consumption and greenhouse gas emissions. Compared to battery electric vehicles (BEVs), an FCV offers long distance mobility and short charging times, which are comparable to today's conventional vehicles. The powertrain system of an FCV is normally designed as a hybrid topology, which combines the fuel cell (FC) with an electric storage unit, like a battery, to power the electric machine. On the one hand, this hybridization brings advantages in performance and fuel consumption by compensating the limited dynamic behavior of the FC system with the battery system and by offering possibilities to store braking energy and to optimize energy flow in the entire drive system. On the other hand, the powertrain becomes a complex structure and so does the design process. Considering the additional options in connection and sizing of the single components, which result in various hybrid topologies, the degree of freedom in the design problem is significantly increased. Furthermore, due to the numerous design criteria depending on specific customer portfolios and the OEMs' desire to introduce their powertrain concepts accordingly, the design process needs to be comprehensive and accurate. The aim is that all customer-related parameters

* Corresponding author. Group Research Powertrain Systems, Volkswagen AG, Letterbox 011/17780, Wolfsburg 38436, Germany. Tel.: +49 5361 9 43035; fax: +49 5361 9 37591.
E-mail addresses: levent.sarioglu@volkswagen.de, leventsarioglu@gmail.com (I.L. Sarioglu).

http://dx.doi.org/10.1016/j.jpowsour.2014.04.135
0378-7753/

are considered and a good customer-product match is assured. This paper presents a design methodology, which considers the above mentioned dependencies and supports the design process at an early stage so that an optimal powertrain design for a hybrid FCV can be determined.

In the following section, the state of art in powertrain design based on the results of the literature survey is presented. We compare various powertrain design methods and evaluate their suitability for this study. In the third section, the proposed methodology is explained. We discuss the modeling of the FCV powertrain and the scalable component models used in the design optimization process. In the fourth section, the results of a case study are presented and discussed. Here, an optimum powertrain design for a typical European long-range passenger vehicle is sought. Finally, the outcomes of this paper are presented in the conclusion section.

2. Literature survey

The design of a vehicle is subject to a wide range of criteria, which are continuously changing since the beginning of the automotive history. There is a long and dynamic list of criteria that a vehicle designer needs to consider. In Ref. [1], these criteria are reviewed and a catalogue of design criteria for vehicles is proposed. In this catalogue, there are seven different main groups of criteria that are classified further into subgroups of two more hierarchy levels, resulting in hundreds of design criteria. However, in this study, those ones related to the conceptualization of an FC powertrain are focused and the catalogue is reduced by excluding the non-relevant criteria for the early phase of a powertrain design. Table 1 concludes the reduced list of design criteria and the four main design objective clusters, namely economic efficiency, driving performance, comfort and environmental impact, which are explained in the following paragraphs.

Basic economic efficiency of a vehicle is found out in conceptualization considering its initial and driving costs. Ref. [2] shows that alone the material and manufacturing costs of a vehicle play a significant role in the suggested retail price of that vehicle. This makes an early cost analysis essential in a powertrain conceptualization. Driving costs depend on the consumption of a vehicle and the price of the energy sources used in that vehicle. These costs may vary with driving style, driving environ (e.g. road, weather and vehicle conditions) and the driven vehicle parameters, as the consumption may vary.

One of the important design criteria for conceptualization of an FC powertrain is driving performance. As listed in Table 1, basic vehicle performance includes maximum driving speed, acceleration performance and climbing ability. A vehicle's maximum speed can differ according to its continuous and peak performance. So called "boosting effect" can help a vehicle drive faster than its continuous maximum speed for a certain duration. The duration of the peak performance in an FCV is mostly limited by the energy capacity of the hybrid storage system or by the overheating of certain components, like the electric machine. On the other hand, acceleration performance of a vehicle is represented typically by the time that is required to accelerate the vehicle from standing state to 100 km h^{-1}. Different speed intervals, such as 60–100 km h^{-1} or 80–120 km h^{-1} can be used to evaluate the vehicle elasticity, as well. Finally, climbing ability is a term to define the maximum grade that the vehicle can drive at a given constant speed.

Table 1
List of design criteria and design objectives for conceptualization of FCV powertrains.

Design criteria	Objective
Economic efficiency	
Driving cost	Minimize
Vehicle cost	Minimize
Driving performance	
Maximum driving speed	Maximize
Acceleration time	Minimize
Climbing ability	Maximize
Peak performance duration	Maximize
Comfort	
Allowed payload	Maximize
Available volume	Maximize
Driving range	Maximize
Environmental impact	
Greenhouse gas emissions	Minimize

Maximum allowed payload, available volume and driving range are important criteria for the comfort of a vehicle. An early volumetric analysis of a powertrain reveals if it basically fits into the intended volume and the unused space can be assumed as the available volume for transport comfort. Similarly, a simple weight analysis finds out if there is free weight capacity that can be used for payload. Finally, the consumption estimation is required to determine the driving range, which also depends on the amount of the energy source that is stored in the vehicle.

Environmental impact of FCVs, which do not emit harmful gases locally, is represented by using global CO_2 emissions due to the fuel production. Commonly used hydrogen generation methods are shown and compared with each other according to their well-to-tank CO_2 emissions in Fig. 1 [3]. Although hydrogen can be produced by using renewable methods without any CO_2 emissions, today the production methods are mostly based on fossil fuels. Therefore the second pathway (450 g kWh^{-1}) is used for well-to-tank analyses in this study.

Considering the above mentioned powertrain design criteria and the increasing complexity of vehicles, the number of corresponding design methods grew significantly over the years. The methods to find out optimum power split between two drivelines concerning fuel economy of a vehicle have been subject to many research topics. The proposed methods vary from non-simulative analytical approaches like the one presented in Ref. [4] to more complex approaches based on advanced vehicle modeling as in Ref. [5]. Among the works about optimization of hybrid vehicles (HVs), especially [6] proposes an effective and accurate approach. The optimization algorithm is run to minimize a total cost function from a financial perspective. However, other relevant vehicle specifications (e.g. driving performance) are not included.

Although HVs with ICE and battery have managed to improve fuel economy in most of the cases, the increasing demand for technologies that use alternative energy sources forces researchers to seek for completely different designs and, hence, design methods. For example, in Ref. [7] components that are based on different technologies are optimized and evaluated as an alternative energy storage system for HVs. Especially the methodology that is developed in Ref. [8] introduces an approach to identify technologies that might have a potential to replace ICE in the next decades for mobility purposes. However, this work focuses on general comparison of today's and tomorrow's mobility concepts, rather than a certain powertrain technology optimization.

In literature, there are numerous new methods to find out optimum FC powertrain concerning the fuel economy. Most of these aim to optimize the energy management strategy. For example, Refs. [9,10] propose universal energy management strategies to reduce fuel consumption, while [11] presents a comparison of the most common energy management strategies for FCHVs with battery. On the other hand, Refs. [12,13] focus on the same research topic for FCHVs with supercapacitors. However, these works focus

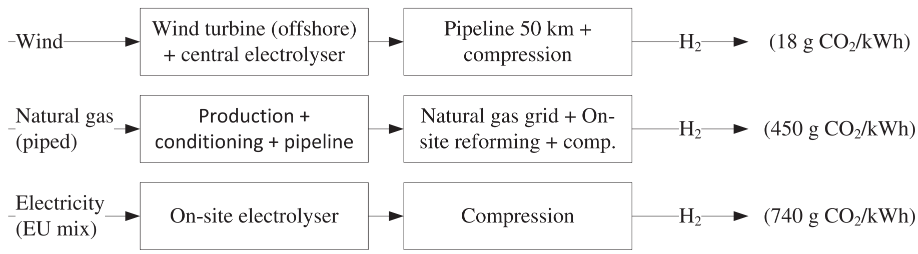

Fig. 1. Selected pathways for hydrogen generation and related CO_2 emissions [3].

on only energy management strategy, which is as important as component sizing in FCV powertrains but not the single aspect. Methods that consider optimization of the energy management strategy together with the sizing of FC system and battery are proposed in Refs. [14,15]. Furthermore, a general design method for a hybrid powertrain, including FCHVs with battery or super-capacitors, is presented in Ref. [16]. Although these works combine the optimization of energy management strategy with scaling of certain components, the fuel economy remains as the single design objective.

Fuel economy and vehicle performance are important vehicle properties. Nevertheless, there are also different criteria (see Table 1) that need to be considered in an FCV powertrain design. A suitable approach that considers various design criteria for evaluation and includes a detailed powertrain modeling that is based on simulation, is presented in Ref. [17] for battery electric vehicles (BEVs). Although the optimization process proposed in this work is remarkable, it is not suitable for FCVs due to the lacking hybrid structure and suitable energy management strategy in the vehicle model.

The survey of existing literature concludes that there is a need for an effective method for conceptualization of FC powertrains. Therefore, a new methodology is developed that considers the effects of component characteristics, powertrain topology choice, sizing of the components, degree of hybridization and energy management strategy on the vehicle properties in order to find out the optimum FCV powertrain concept according to the design objectives that are related with customer's decision making.

3. Methodology and design case study

In this section, we present the methodology in a case study to find out the optimum conceptual design of an FCV powertrain. It is important to note that the parameter assumptions made in the following design problem do not represent any real vehicle or component. However, they represent realistic values based on experience, modeling and literature.

The overall design process starts with establishing the design requirements and conditions. In addition to the general design objectives (see Table 1) from literature, Table 2 lists quantitative design constraints specific to this case study. They include the desired base vehicle, estimated accessories consumption and the minimum requirements for an assumed typical mid-size European long-range vehicle. In this paper, the term "base vehicle" refers to all parts of an FCV except its powertrain. The wheels, braking system and driving axles are also included in base vehicle, since they are assumed not to be varied with powertrain. Base vehicle is defined by using a set of parameters, which are mostly essential in longitudinal dynamics of the vehicle. These parameters include vehicle air drag coefficient c_W, vehicle frontal area A, rolling friction coefficient f_r, dynamic wheel radius r_{dyn}, base vehicle mass m_{base}, moment of inertia of rotating parts (e.g. wheels, break discs and axles) J_{base}, base vehicle drive efficiency (e.g. differential and wheel bearings) η_{base}, available volume for powertrain $V_{base,av}$, and manufacturing cost of the base vehicle C_{base}.

The average accessories consumption is relevant for energy consumption and is assumed to have a relatively high value, considering the increasing trend, whereas the maximum accessories consumption is relevant for the driving performance. The minimum requirements given for the maximum driving speed, acceleration time and driving range are average results of a questionnaire among multiple powertrain experts. The resulting powertrain design is expected to fulfill not only the given design requirements but also general expectations, such as minimum cost, minimum environmental impact, maximum vehicle performance and maximum comfort. Considering the variety of these expectations, a single ultimate best solution is not expected and a trade-off analysis is necessary for the decision making. In order to achieve this, a large search space needs to be swept and calculated accurately.

In order to define the search space, the design variables, their ranges and the initial number of variables with resulting step sizes are summarized in Table 3. A certain number of values are chosen

Table 2
Established design requirements for a typical long-range vehicle.

Base vehicle	B-Segment
c_W, A, f_r, r_{dyn}, m_{base}, J_{base}, η_{base}, $V_{base,av}$, C_{base}	0.3, 2.22 m^2, 0.008, 0.3 m, 1300 kg, assumed 3% of m_{veh}, 0.98, 500 l, 8 k€
Accessories consumption	
Average and Maximum	850 W and 5000 W
Weight	
Payload capacity (excl. 75 kg driver)	400 kg
Average payload (for consumption)	200 kg
Maximum allowed total weight	2475 kg
Minimum requirements	
Maximum continuous driving speed	172 km h^{-1}
0–100 km h^{-1} acceleration time	10.2 s
Driving range	520 km
Duration of peak driving performance	30 s

Table 3
Design variables, their numbers, discrete step sizes and the size of the search space.

	Variable	Scope	Number	Step size
Powertrain topology	Topology	Topologies A, B, C & D	4	N/A
FC system power rating	P_{FC}	Min. 10 kW; max. 150 kW	25	5.83 kW
Battery power rating	P_{batt}	Min. 0 kW; max. 150 kW	25	6.25 kW
Battery energy capacity	E_{batt}	Min. 0 kWh; max 6 kWh	20	0.32 kWh
Hydrogen storage capacity m	m_{H_2}	Min. 2 kg; max. 7 kg	10	0.55 kg
Electrical machine power rating	P_{EM}	Min. 60 kW; max. 110 kW	15	3.57 kW
Total number of combinations in the search space: 7.5 × 10^6				

for each variable and they are linearly spaced between their given maximum and minimum, leading to a constant step size. The size of the search space is calculated by multiplying the number of all variables, due to the simple combinatorics that is used in generating the FCV combinations.

A relatively wide scope of component sizing is chosen due to the uncertainty at the beginning of the design progress. The discrete step size plays a crucial role in accuracy and computational efficiency of the methodology. Large steps with low number of variables in component scaling would result in a very rough resolution in the search space and reduce the accuracy of the design process. On the other hand, a very fine resolution with high number of variables would reduce computational efficiency. Therefore a moderate choice is preferred at the beginning of the design process.

The most common FC powertrain topologies are shown in Fig. 2. The topologies A and B belong to pure fuel-cell vehicles (PFCVs), while the topologies C and D belong to FCHVs. All topologies include an electric machine module, which includes the required inverter and the gear system, an FC system and 12 V vehicle accessories, which are connected through a DC/DC converter to the high voltage DC bus. In topologies A and C, the DC bus voltage is determined by the FC voltage output and it fluctuates during driving. The main advantage of this situation is the lacking DC/DC converter losses between the main energy source, namely the hydrogen tanks, and the electric machine. On the other hand, topologies B and D offer a solution with a constant high voltage at DC bus. This is possible in a hybrid powertrain by using a three-port DC/DC converter, which is theoretically a combination of two DC/DC converters on both FC system and battery sides. A three-port DC/DC converter causes additional losses, weight, volume and cost in powertrain but the constant DC bus voltage may increase the overall efficiency of the electric machine. Besides the components connected to the DC bus, like the FC system components and the electric machine, can be designed considering a high constant DC bus voltage. Therefore a reduction in cost, weight and size of these components can be expected. This improvement is assumed as overall 10% at the first step.

The variation of the component sizing requires the variation of component characteristics. Therefore, scalable component models that deliver the characteristics data of the components are necessary. Although it is possible to estimate these characteristics of the components of various sizes by using detailed simulation models, it becomes unfavorable, when calculation efficiency is a concern. Some detailed scaling methods are shown in Ref. [16] for FC systems and in Ref. [18] for various powertrain components. However, these methods mostly require comprehensive component knowledge. Therefore, a simpler, but for optimization sufficiently accurate, modeling approach is followed. In order to define a universal method for all of the components, a method, which is based on linear interpolation between characteristics data of given sample components, is used. By doing so, a continuous scaling of components according to their basic parameters is realized. For each component model, at least two sample components of different sizes are provided with specific characteristics data, so that the nonlinear effects in scaling can be partially included, as well. The data for these sample components do not represent existing components; instead they are obtained through assumptions in combination with modeling. However, they are compared with available real component values in literature to assure the validity of the results. The assumed characteristics for each component are presented in the following parts.

3.1. Modeling of fuel-cell system

Data of four sample FC systems with different power ratings (P_{FC}) are used for continuous scaling based on linear interpolation. The assumed specific values (on primary vertical axes and denoted with lower-case symbols) and the resulting weight, volume and cost (on secondary vertical axes and denoted with upper-case symbols) are shown in Fig. 3 over the scaling range. Additionally, it is possible to find some reference values, which are published in internet by mostly FC system manufacturers in form of datasheets. For example, the FC systems HyPM-HD16 and HyPM-HD30 from the manufacturer Hydrogenics [19] and Hy-80 from NuCellSys [20] show that our weight and volume modeling is realistic. For a higher power segment the FC system from GM Equinox [21] is included only in the first plot, since no volumetric value is provided. Similarly, it is also difficult to find price data of existing FC-systems. Nevertheless, in Ref. [22] the results of an extensive cost analysis of McKinsey with several OEMs about their FCVs are reported. These values are plotted in order to verify the cost modeling.

In order to calculate the FC-system losses in a driving cycle accurately, a modeling approach that is based on overall efficiency curve over operating range is followed. The continuous scalability is assured based on linear interpolation between various curves. Fig. 4 shows four sample system efficiency curves with the

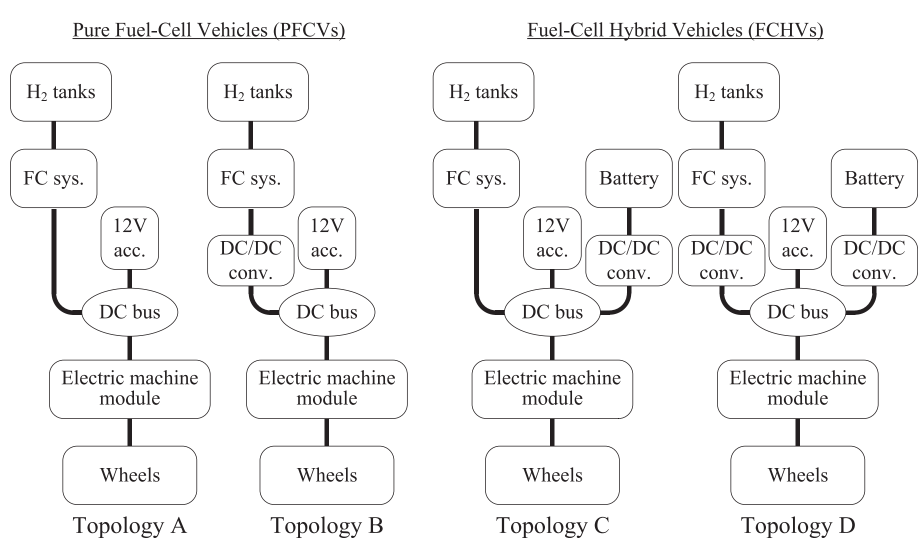

Fig. 2. Most common PFCV and FCHV powertrain topologies.

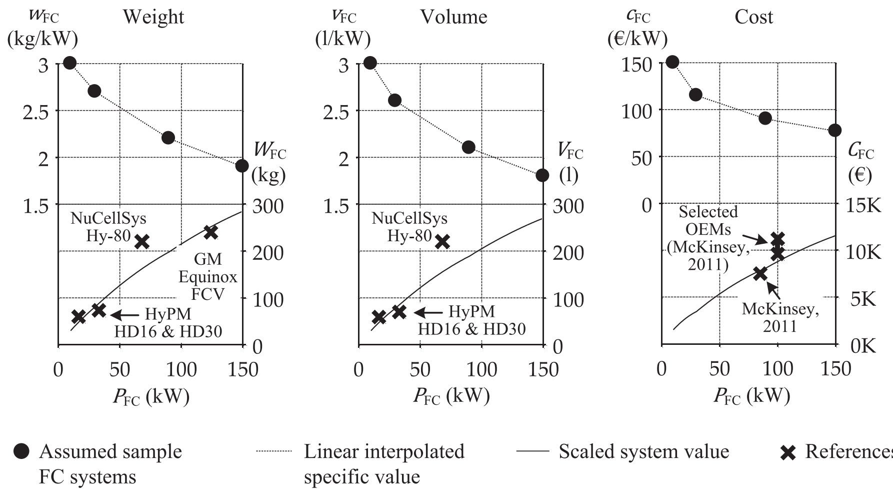

Fig. 3. Specific values of the assumed sample FC systems and the resulting system weight, volume and cost.

horizontal axis representing the normalized FC system power output. These sample curves are obtained by using a detailed FC-system model and provided for this case study. It is important to note that the shapes of the resulting curves are similar to the most of the real FC-systems, some examples of which are shown in Ref. [23]. For further scaling of the FC system with an intermediate desired power rating, a new normalized efficiency curve is obtained based on simply the linear interpolation between these sample curves.

3.2. Modeling of battery

System based energy specific values of four sample battery cells as well as the power rating and energy capacity of the resulting batteries are shown in Fig. 5. In order to realize a continuous battery scaling, the battery model uses the given sample battery cells, and interpolates between two cells according to the desired power-to-energy ratio. However, in cases, where the power-to-energy ratio is higher or lower than the ratios of the given samples, the boundary cells are used. According to the given specific values and based on linear interpolation method, the weight, volume and cost of a battery with desired energy capacity and power rating can be estimated. In order to verify the assumed cell parameters, three real battery systems of different applications are included in the table next to the plot. These include a typical HEV battery pack with a high power-to-energy ratio from the manufacturer Cobasys [24], the PHEV battery pack with an intermediate power-to-energy ratio from Toyota Prius [25] and the EV battery pack with the lowest power-to-energy ratio from Nissan Leaf [26].

About the cost of battery systems there are many energy specific values in literature. These can be as low as \$400 kWh^{-1}. However [22] shows that OEMs are far from these low values with their FCV concepts. We make a higher assumption with a more realistic approach by considering the following two aspects in these low values. Firstly, the low values are mostly based on very high number of production rates (>200 K year^{-1}). Secondly, the effect of varying power-to-energy ratio on energy specific price is most of the time ignored. Therefore we assume an increasing energy specific price as the power-to-energy ratio of the battery system increases.

In addition to the weight, volume and cost of a battery system, the losses in the battery are also required for vehicle simulations. Among the electrochemical, mathematical and electrical modeling approaches, the electrical modeling that is based on the equivalent circuit models is commonly used to represent the transient and steady state behavior of battery systems. The choice of the appropriate electrical battery model depends highly on the application. For example, transient characteristics and the electrochemical process are represented better in equivalent circuit models based on impedance spectroscopy. Since the battery transients are not of high importance in the conceptualization design step, a basic internal resistance electrical battery model, in which the cell open circuit voltage and inner resistance are represented, is chosen to determine the efficiency of the battery systems in the search space. According to this, the potential difference at a battery cell terminal can be shown as:

$$U_{\mathrm{cell}} = U_{\mathrm{oc,cell}} - R_{\mathrm{in,cell}} \times I_{\mathrm{cell}}$$

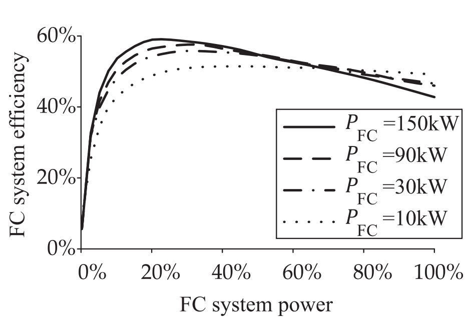

Fig. 4. System efficiency curves of four FC systems with different power ratings, used as samples in scalable FC system model.

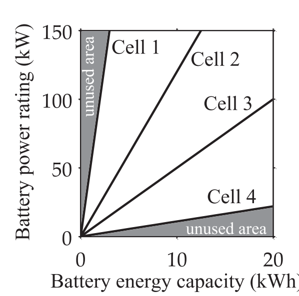

	P_{batt}/E_{batt} (kW/kWh)	w_{batt} (kg/kWh)	v_{batt} (l/kWh)	c_{batt} (€/kWh)
Cell 1	50	55	19	3900
Cell 2	12	27	15	1500
Cell 3	5	17	13	1000
Cell 4	1.1	9	10	680
NiMHax HEV	*25*	*45.9*	-	-
Prius Plug-in	*14*	*18.2*	-	-
Nissan Leaf	*~3.7*	*12.5*	-	-

Fig. 5. Battery power rating, energy capacity and specific values of assumed four different battery cells.

where $U_{\mathrm{oc,cell}}$ is the cell open circuit voltage $R_{\mathrm{in,cell}}$ is the cell internal resistance, and I_{cell} is the battery cell current. Furthermore the efficiency of the battery cell can be given as:

$$\begin{cases} \eta_{\mathrm{cell}} = \dfrac{U_{\mathrm{cell}}}{U_{\mathrm{oc,cell}}}, & I_{\mathrm{cell}} \geq 0 \\ \eta_{\mathrm{cell}} = \dfrac{U_{\mathrm{oc,cell}}}{U_{\mathrm{cell}}}, & I_{\mathrm{cell}} < 0 \end{cases}$$

where the open circuit voltage and internal resistance vary depending on the SoC of the battery cell. Typically battery cell efficiencies are above 85%, unless they have a very low SoC and high current output [27]. Fig. 6 shows the resulting efficiency curves of Cell 1 and Cell 4 as a function of depth of discharge (1-SoC). The parameters of these sample battery cells are assumed based on measured data of real high-power and high-energy battery cells. The efficiency curves for a desired battery cell with an intermediate power-to-energy ratio are calculated by using cell parameters that are estimated by linear interpolation between the sample cells.

3.3. Modeling of hydrogen storage tank system

The hydrogen storage tank model is designed to deliver characteristics of a storage system with a desired hydrogen capacity $m_{\mathrm{H_2}}$. Fig. 7 shows three assumed sample systems with different storage capacities and specific weight, volume and cost according to their storage amounts. In order to achieve a continuous scaling, the specific values for intermediate values are obtained through linear interpolation. The resulting system weight, volume and cost curves can also be seen on the secondary vertical axes at each plot. In addition to our modeling results, reference systems are plotted for verification. Ahluwalia et al. [28] shows a comparison of various hydrogen storage systems, including tank systems with two high pressure (70 MPa) cylinders, which are shown in both plots. The significant difference between their results and our modeling in volume can be explained with a compact balance of plant and more efficient use of the space with higher number of cylinders in our assumption. Finally, cost analyses of hydrogen tank systems from McKinsey [22] and Strategic Analysis [29] show that the cost assumptions are realistic.

Despite the minimum amount of losses due to the hydrogen flow through valves and pipelines in hydrogen storage tanks, the on-board efficiency of hydrogen tanks is assumed to be 100%.

3.4. Modeling of electric machine unit

The electric machine is modeled as a module including a DC/AC inverter unit and a single-ratio transmission unit. The mechanical power rating P_{EM} of the module is considered as basis for scaling. In order to calculate the weight, volume and cost of the scaled system, the assumed specific values of three sample electric machine modules with different power ratings are used. Fig. 8 summarizes these values and the resulting scaling curves. Since the EM module is modeled as unit with EM, inverter and the gearbox, it is difficult to find a comparable reference module, with published weight and volume specifications in literature. Therefore a verification of weight and volume modeling based on real components is not possible. However, [22] reports the questionnaire conducted by McKinsey about the cost estimates of several FCV OEMs for such EM modules. The average of OEMs' estimations for a certain power segment range, which intersects our cost model, is shown in the last plot, as well.

An electric machine module is a nonlinear complex system and its losses depend on not only the type and size of the components but also the operating conditions. Therefore normalized characteristics maps of sample electric machine modules with different power ratings are employed. Three examples of these maps only with driving operating points (first quadrant) are shown in Fig. 9. These maps are obtained for this case study as a result of detailed FEM-based analyses, due to the lack of real data. For the verification of these sample maps, it is important to note that the distribution of losses depending on operating point is similar to the measured data, presented in Ref. [30]. In order to achieve a simple continuous scaling, linear interpolation method is used to generate new normalized characteristics maps for the electric machine modules with desired power ratings between the provided power ratings.

3.5. Modeling of DC/DC converter

The power ratings of DC/DC converters are varied depending on their neighboring components. A DC/DC converter in a vehicle powertrain is relatively small, light, cheap and high efficient compared to the FC system or a battery. Therefore a relatively simple scaling model for the DC/DC converters are developed by assuming constant specific weight of 0.23 kg kW^{-1}, constant specific volume of 0.13 l kW^{-1}, constant specific cost of 8 € kW^{-1} and constant efficiency. These devices are mostly capable of performing with efficiency higher than 97%, even under fluctuating DC bus voltage, with the help of implementing soft-switching techniques and using silicon-carbide semiconductor devices. Although there might be extreme cases, especially in PFCV topologies, where the voltage output of the FC system decreases and the losses in DC/DC converter increase for a short time, a constant value of 97% for efficiency is used in this case study for simplicity.

3.6. Energy management strategy and powertrain model

Defining a suitable energy management strategy is as crucial as component sizing in powertrain design. The task of the energy

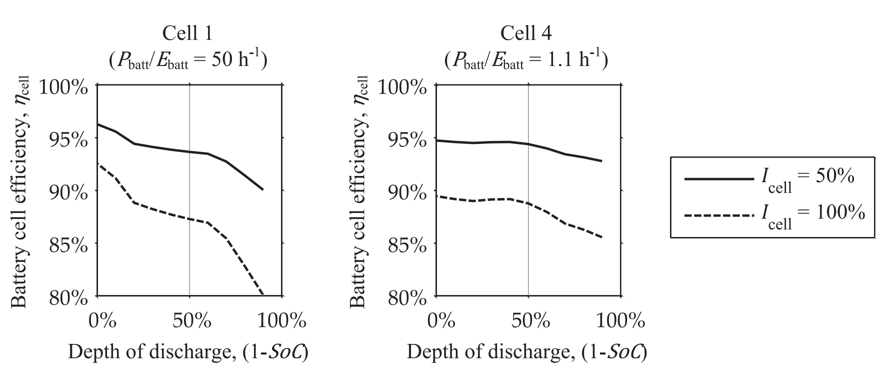

Fig. 6. Calculated efficiency curves for battery cells 1 and 4.

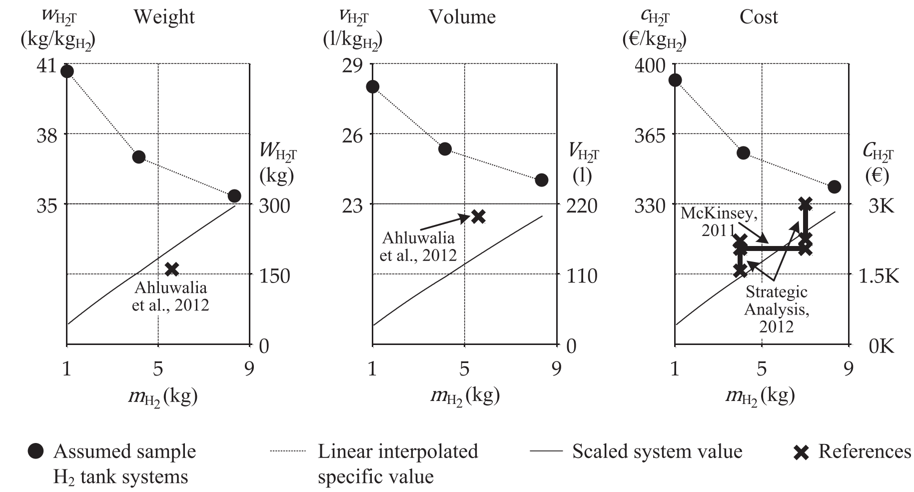

Fig. 7. Specific values of the assumed sample H_2 tank systems and the scaled system weight, volume and cost.

management is the coordination of the power flow in the powertrain system. Assuring the drivability of the vehicle, reproducibility of the peak performance and sustaining the lifespan of the components combined with high driving efficiency are the major tasks of the energy management strategy. The Adaptive Load Strategy (ALS) described in Ref. [10] is a universal and adaptive energy management strategy, which can be used for all of the FCVs and in all driving conditions that are considered in conceptualization, and assures an optimum energy flow in the powertrain every time.

The powertrain model plays a crucial role by calculating the vehicle performance and energy consumption in a given driving pattern. It needs to deliver accurate results by taking into account varying component losses and energy flow in the driving cycle. Therefore, we propose a validated and simulation-aided powertrain model. The model is able to read above defined component specifications and simulate the power flow in the drivetrain by following a given driving cycle. The validation of this model is done by simulating and measuring an existing Volkswagen FCHV with known detailed component specifications. In this validation, the attention is given to that the error between simulated and measured amount of utilized energy at output and input of each powertrain component during a drive pattern does not exceed 2.5% at any time.

In this part, it is important to mention the difficulties in validation of design methodologies. The results of a design methodology, in this case the optimum design of a vehicle powertrain, change significantly depending on design constraints, objectives and used evaluation methods, even if the input data of used powertrain models remain unchanged. Without knowing exact component specifications, design objectives, evaluation parameters and several other variables, it is not possible to compare the results of this methodology with an existing vehicle design, which is a result of a completely unknown another design process.

4. Results and discussion

A large solution space is obtained after all FCV combinations in the search space are analyzed. However, visualization of the multidimensional results of such a rich solution space is complicated. Parallel coordinates method [31] offers a compact way of visualizing and comparing such multidimensional data without any limitation in number of parameters that are to be visualized. This method uses parallel axes for each parameter and represents each solution with a polyline connecting the axes from the corresponding values. In case of very high number of plotted solutions, the polylines might form a solid picture and cannot be

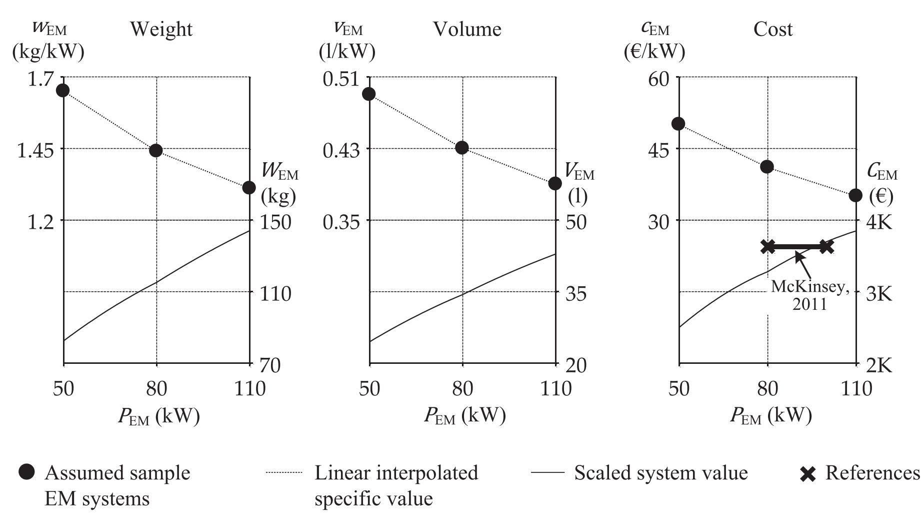

Fig. 8. Specific values of the assumed electric machine module samples and the scaled system weight, volume and cost.

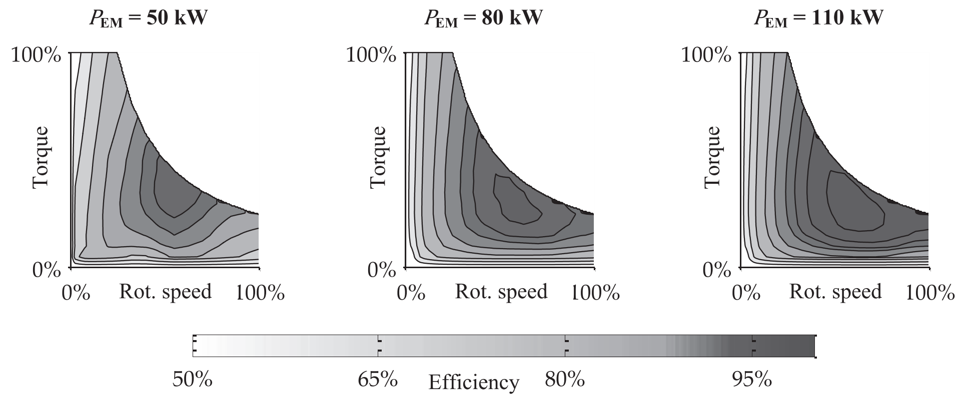

Fig. 9. Estimated characteristics maps of electric machine module samples that are used for the scalable model.

differentiated from each other. However, by highlighting certain groups of the solutions, these plots show certain trends and trade-offs in solutions, which is aimed in this paper.

Due to the simplicity of combinatorics in definition of the search space, the solution space includes also many nonsensical FCV combinations. Therefore, there is a high potential in reducing the size of the solution space before going to the next step, where the evaluation takes place. Fig. 10 shows the solution space by using a parallel coordinates plot with fourteen axes, each representing a different parameter. The combinatorics in definition of the search space is seen obviously in the first six axes, which represent the design variables, while the rest of the axes include certain vehicle specifications, such as 0–100 km h^{-1} acceleration time, maximum continuous driving speed, climbing ability at 60 km h^{-1}, hydrogen consumption in NEDC, driving range, total vehicle weight (including 200 kg payload and the powertrain), powertrain volume and powertrain cost. The minimum and maximum values on the axes show that the solution space includes FCV combinations with vehicle properties changing significantly. These combinations are reduced by applying two filtering steps, and the remaining combinations after each filtering step are shown with dark gray and black, respectively. Firstly, it is possible to see all of the results with the lightest gray tone, which also includes FCV combinations that do not make any sense from the design point of view. For example, the combinations that achieve only around 10 km h^{-1} maximum continuous driving speed or have a driving range of less than 150 km or accelerate from zero to 100 km h^{-1} in more than a minute are also in the solution space. Therefore, in the first filtering step the minimum requirements are compared with each solution. These include the requirements for maximum continuous driving speed, acceleration time, driving range and peak performance duration, which are shown in Table 2. Additionally, the drivetrain needs to fit into the available space in base vehicle and weigh less than the allowed limit. Applying these limitations in the first filtering step leads to a considerable reduction in the solution space. Looking at the diagram it is possible to conclude various results, concerning the effects of minimum requirements on the powertrain design. For example, the requirement for the maximum continuous driving speed leads to the election of the FCV combinations with FC systems under a certain power rating. This automatically leads to that the combinations with a low climbing ability are filtered out, as well. The solutions with topologies A and B, which do not have an additional power source like a battery, require an FC system with comparably higher power rating around 110 kW in order to fulfill the given performance requirements, whereas the hybrid solutions with topologies C and D require a minimum FC system power rating around 70 kW. Similarly, the minimum driving range and maximum acceleration time limits lead to the election of the FCV combinations including a hydrogen tank system with a capacity under around 4 kg and an electric machine with a power rating under around 85 kW, respectively. On the other hand, the upper limitation concerning the powertrain volume and vehicle weight leads to the election of the expensive FCV combinations that combine an over-sized FC system and a battery at the same time.

In the second filtering step, the FCV combinations are compared with each other according to the domination principle [32]. According to this, when an FCV is worse in all properties than any

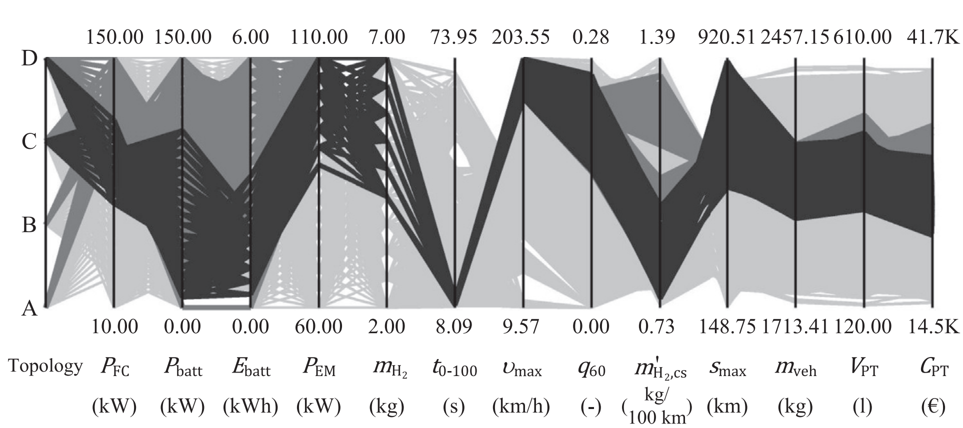

Fig. 10. Results of filtering the solution space with selected technical vehicle specifications.

other FCV in the remaining feasible solution space, then it is "dominated" by another one and there is no need to keep it for a further evaluation. At the end of this process, the number of remaining combinations in the solution space is reduced further. Especially the combinations without a battery (Topology A and B) are excluded at this step. These combinations are eliminated since they are dominated by other combinations with hybrid powertrains. It is also seen that over-dimensioning the FC-system above approx. 110 kW or the battery power rating and the energy capacity greater than approx. 110 kW and 2.6 kWh does not bring any advantages for the vehicle properties. These solutions are dominated by the combinations with FC systems and batteries that are dimensioned according to the electric machine module and used hybrid functions. The remaining solution space is called non-dominated feasible solution space, since its members are non-dominated and fulfill all of the design requirements and conditions. The following part explains how the decision making is supported in order to reach a single solution among the non-dominated feasible solution space.

Fig. 11 shows the remaining non-dominated feasible solution space after the filtering. Unlike the previous diagram in Fig. 10, there is no highlighted group of solutions, just the minimum and maximum values of the axes. However, note that some of the technical vehicle specifications in Fig. 10 are converted to customer-relevant vehicle specifications before they are shown in Fig. 11. For example, instead of hydrogen consumption m'_{H_2cs} in NEDC, the driving costs $C_{d,NEDC}$ are calculated and shown. This is achieved by simply multiplying the hydrogen cost, which is assumed as 9.5 € kg^{-1}, with the hydrogen consumption rate. Similarly, the allowed payload weight $m_{load,max}$ and available free volume V_{av} in Fig. 11 are calculated by using vehicle's total weight m_{veh} and powertrain volume V_{PT} in Fig. 10. Finally, instead of powertrain costs C_{PT}, the total vehicle cost C_{veh}, as the sum of the cost of base vehicle and powertrain, is shown in Fig. 11. Considering the wide range of values in vehicle specifications, it becomes obvious that there is not an ultimate best solution with best values in all axes. In other words, it would be not realistic to expect a solution that fulfills all of the design objectives, such as maximum driving range and performance with minimum costs, at the same time. Therefore, a detailed look at trade-offs between the design objectives is necessary.

A trade-off analysis does not aim to identify an optimum solution, directly. It is used to show and quantify the changes in other vehicle specifications, when a certain vehicle specification is improved. Also in the following, a certain powertrain design is not selected, but it is shown what is necessary in order to maximize or minimize a desired vehicle specification.

The parallel coordinates method with an interactive brushing (highlighting) offers a suitable visual technique for the trade-off analysis. In Fig. 12, there are three example screenshots, each time with a different group of solutions brushed according to the desired vehicle specification. By brushing only the combinations that fill a certain criteria with a parameter, it is clearly seen how the other parameters of these combinations change. For example, in the first diagram it is possible to see that the maximum continuous vehicle speed v_{max} is desired to be maximized (above 200 km h^{-1}) and therefore only these combinations are brushed. As it can be seen, small increases in acceleration time, driving costs and vehicle costs are expected. But more significant reductions need to be expected in allowed payload weight and volume. In the second diagram, the solutions with a maximum driving range (>900 km) are brushed. Other parameters of the brushed combinations show that the maximum driving range results in slight decreases in climbing ability and acceleration performance. More significant losses are also expected in vehicle cost, allowed payload weight and volume. Finally, the brushed solutions with minimum vehicle cost show that there is a strong trade-off between the vehicle cost and the other specifications, like driving range and acceleration performance. The allowed payload weight and volume, on the other hand, change positively with reducing vehicle cost.

Although visual methods for trade-off analysis give a good overview about the relationship between vehicle specifications, Table 4 is included in order to provide a quantitative analysis. For each vehicle specification, the best FCV solution is selected (best values are highlighted in bold for each FCV) and checked how its rest values change in comparison to the minimum and maximum values in the non-dominated feasible solution space. In order to compare the changes in different vehicle specifications, they need to be normalized by using a proper scoring method. Various non-linear functions can be applied for scoring certain vehicle specifications. However, when there is no detailed knowledge about the influences of changes, the linear scoring method offers a simple and objective way for normalizing, especially within the non-dominated feasible solution space. For the linear scoring, two non-existing FCV solutions, which are simply the combinations of only the best and only the worst specification values in the non-dominated feasible solution space, are assumed. These imaginary solutions are called the ultimate best FCV and the ultimate worst FCV, and form the basis for the linear percentage scores shown in Table 4. These scores are calculated according to the absolute values in parentheses as a result of a simple linear function between the corresponding worst and best values. This is why the ultimate best

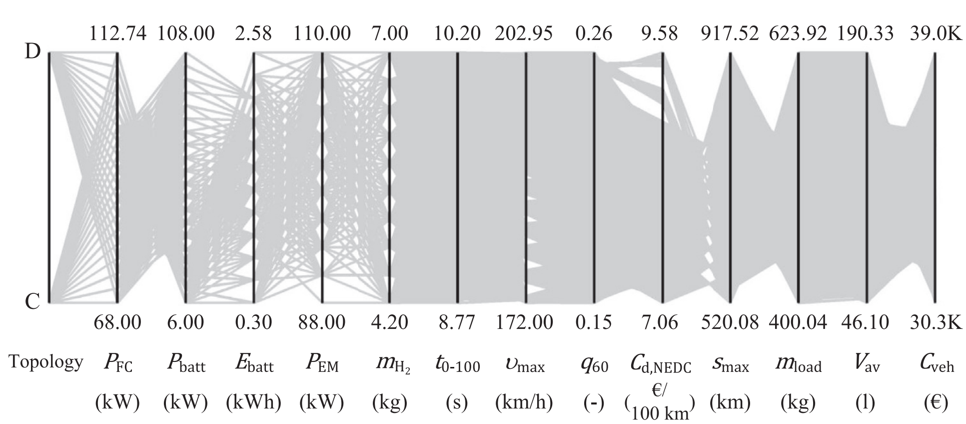

Fig. 11. Non-dominated feasible solution space with some of the selected customer-related vehicle specifications.

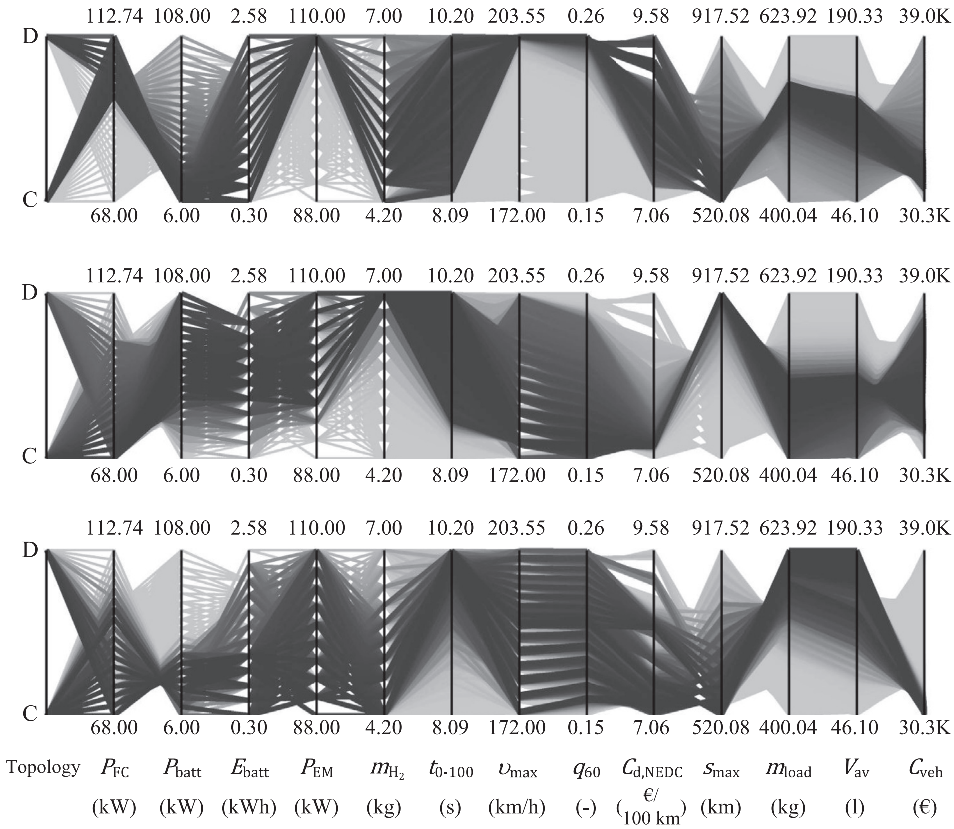

Fig. 12. Multiobjective trade-off analysis by using parallel coordinates method with brushing technique. Maximum continuous driving speed, maximum driving range and minimum vehicle costs are desired in the first, second and third pictures, respectively.

FCV is scored with 100% overall, whereas the ultimate worst FCV with 0%.

Some of the interesting conclusions from the quantitative trade-off analysis are as follows:

- There is no real ultimate best FCV solution.
- The lowest driving costs in NEDC come with significant disadvantages in driving range (11%), maximum driving speed (11%) and acceleration time (5%).
- The lowest vehicle cost is only possible in cost of driving range (9%), maximum driving speed (22%) and acceleration performance (2%).
- The FCV with the highest driving speed has a driving range score as low as 5%, and a low carbon dioxide emissions score of 43%. This can be explained by the lack of extra hydrogen tanks and hybridization in order to save weight.
- The FCV with the best acceleration performance has almost the worst continuous driving performance with 1% maximum driving speed.
- The highest payload capacity is possible, only if the driving range and driving performance scores are reduced to below 11%.
- Apparently, the necessary hydrogen storage system for the highest driving range uses the available payload weight capacity and space, which are reduced to 36% and 44%, respectively.

As it is seen, the non-dominated feasible solution space does not include a solution that has the best values in all vehicle specifications. Given this situation, one way to reach a single

Table 4
Results of the trade-off analysis by selecting the best FCV concepts according to each vehicle specification. Percentage values based on a linear scoring between the ultimate best FCV and the ultimate worst FCV and the absolute values in parentheses.

	$C_{d,\mathrm{NEDC}}$ (€/100 km)	C_{veh} (€)	$v_{\mathrm{max,cont}}$ (km h^{-1})	t_{0-100} (s)	$m_{\mathrm{load,max}}$ (kg)	V_{av} (l)	$s_{\max}$ (km)	E_{CO_2} (g km^{-1})
Ultimate best FCV[a]	100% (7.1)	100% (30.3 K)	100% (202.9)	100% (8.8)	100% (623.9)	100% (190.3)	100% (917.5)	100% (111.4)
FCV with best $C_{d,\mathrm{NEDC}}$	**100% (7.1)**	80% (32.1 K)	11% (175.5)	5% (10.1)	83% (584.9)	90% (176.6)	11% (564.8)	100% (111.4)
FCV with best C_{veh}	95% (7.2)	**100% (30.3 K)**	22% (178.7)	2% (10.2)	93% (608.9)	93% (180.0)	9% (554.8)	95% (113.4)
FCV with best $v_{\mathrm{max,cont}}$	43% (8.5)	93% (31.0 K)	**100% (202.9)**	24% (9.9)	70% (557.5)	57% (127.9)	5% (539.1)	43% (134.1)
FCV with best t_{0-100}	92% (7.3)	71% (32.9 K)	1% (172.4)	**100% (8.8)**	78% (574.3)	90% (175.7)	7% (549.2)	92% (114.6)
FCV with best $m_{\mathrm{load,max}}$	92% (7.3)	100% (30.4 K)	2% (172.6)	1% (10.2)	**100% (623.9)**	100% (190.3)	7% (549.2)	92% (114.6)
FCV with best V_{av}	92% (7.3)	100% (30.4 K)	2% (172.6)	1% (10.2)	100% (623.9)	**100% (190.3)**	7% (549.2)	92% (114.6)
FCV with best $s_{\max}$	93% (7.2)	64% (33.5 K)	9% (174.9)	4% (10.1)	36% (479.7)	44% (109.1)	**100% (917.5)**	93% (114.3)
FCV with best E_{CO_2}	100% (7.1)	80% (32.1 K)	11% (175.5)	5% (10.1)	83% (584.9)	90% (176.6)	11% (564.8)	**100% (111.4)**
Ultimate worst FCV[a]	0% (9.6)	0% (39.0 K)	0% (172.0)	0% (10.2)	0% (400.0)	0% (46.1)	0% (520.1)	0% (151.0)

[a] Non-existing, imaginary solutions.

solution is to define weighting factors for each design objective and generate a linear objective function. In order to do this, the vehicle specifications, which are subject to a design objective, are clustered according to [1]. These clusters and the design objectives can be seen in the weighted objectives tree that is shown in Fig. 13.

The weighting factors in the tree are based on a questionnaire among five powertrain experts. The aim of the questionnaire was to find out subjective values of each design objective, from the perspective of a powertrain expert. Each expert is asked to give a value from 0 to 10 of all vehicle specifications that are subject to design objectives. Then, simply, the average of all values from different experts is used to calculate the weighting factor of a specific design objective based on its cluster. It must be noted that the resulting weighting factors include subjectivity of a certain group of people, based on their knowledge, experience and personal preferences. Therefore the standard deviation in the answers of the asked experts can be used as an indicator of subjectivity. According to this, the design objectives maximizing driving range and minimizing the vehicle costs have a relative standard deviation below 10%. On the other hand, the relative standard deviation increases up to 40% for the design objective minimizing the driving costs in the city. In average the relative standard deviation for all design objectives equals to 20%, which is acceptable, considering the low number of questionees.

The next step after creating the weighted objective tree is to find out which solution fulfills which design objectives at which rates. In order to do this, the suitable linear scoring technique from the previous section is used. In other words, each vehicle specification of each candidate solution is compared with the corresponding worst and best values in the non-dominated feasible solution space and a score in percentage is assigned. Finally, the solution that collects the maximum weighted score, based on the given weighted objective function, is assumed to be the optimum solution. According to this, the optimum solution as a result of this analysis is the hybrid powertrain that is shown in Fig. 14.

The identified optimum powertrain for a typical long-range FCV is a hybrid powertrain based on Topology C, which includes a DC/DC converter on the battery side. It is composed of hydrogen storage tanks with approx. 4.2 kg storage capacity, which is just enough amount of hydrogen necessary for the minimum required driving range. Its FC system delivers maximum approx. 71 kW, which is slightly more than the necessary power to drive the vehicle around its required continuous maximum driving speed. The battery's power rating of 54 kW, combined with 110 kW peak power rating of the electric machine, provides the drivetrain the extra power, resulting in a relatively good peak driving performance. On the other hand, its energy capacity is not so much to supply a long-standing peak driving performance duration, but 1.1 kWh is enough for the required 30 s of peak performance duration and most of the hybrid functions to increase the efficiency of the drivetrain. All these factors sum up to a maximum weighted score greater than 70%, where 100% would mean the ultimate best and 0% the ultimate worst. It is also important to note that the less the trade-offs in the solutions are, the closer the scores to 100% are. This is why; the maximum score of the optimum solution might also be used as a general indicator for the trade-offs in the non-dominated feasible solution space.

Knowing the weighted scores of all solutions in the non-dominated feasible solution space provides the basis for a sensitivity analysis. Plotting the weighted scores vs. powertrain design variables helps understanding the design trends. Fig. 15 includes five different scatter plots with their vertical axes representing the weighted score and their horizontal axes representing a different

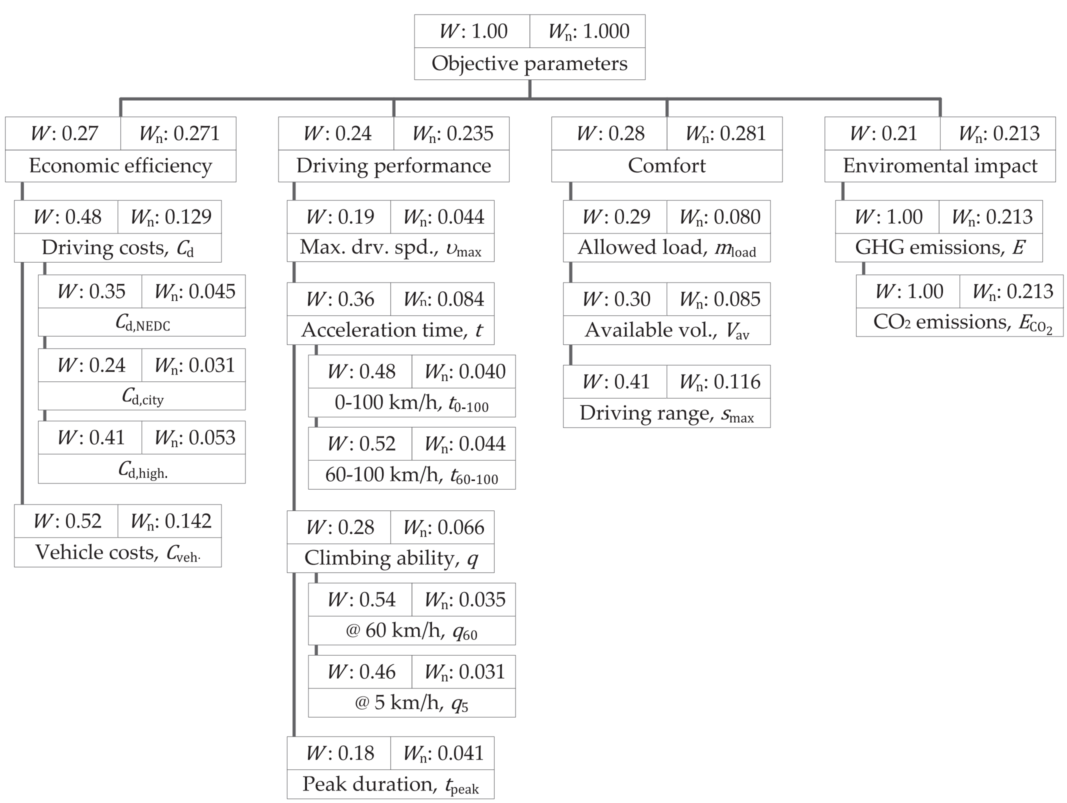

Fig. 13. Weighted objective tree, where W represents the weighting factor of the design objective in the same hierarchy level and W_n is the normalized weighting factor with respect to the highest level.

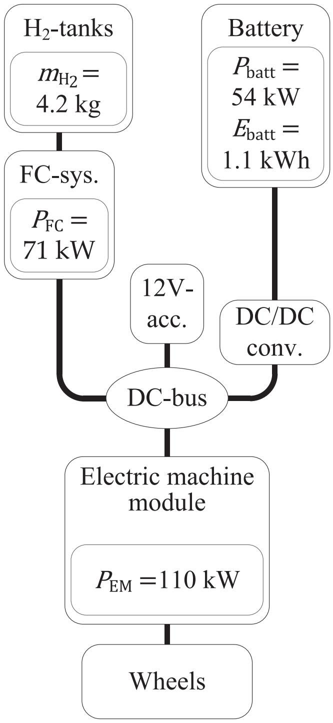

	Unit	Value	Score, S	W_n	$S\times W_n$
$C_{d,NEDC}$	€/100km	7.1	96.8%	0.045	4.4%
$C_{d,city}$	€/100km	9.8	93.5%	0.031	2.9%
$C_{d,high.}$	€/100km	9.7	95.5%	0.053	5.1%
C_{veh}	€	32.2K	79.7%	0.142	11.3%
$\upsilon_{max,cont}$	km/h	178.7	21.7%	0.044	0.9%
$t_{0\text{-}100}$	s	8.8	96.3%	0.040	3.9%
$t_{60\text{-}100}$	s	4.7	96.1%	0.044	4.2%
q_{60}	-	0.2	23.8%	0.035	0.8%
q_5	-	1.0	100.0%	0.031	3.1%
t_{peak}	s	31.2	1.5%	0.041	0.1%
$m_{load,max}$	kg	574.9	78.1%	0.080	6.3%
V_{av}	l	171.5	87.5%	0.085	7.4%
s_{max}	km	558.5	9.7%	0.116	1.1%
E_{CO_2}	g/km	112.7	96.8%	0.213	20.6%
					$\sum = 72.1\%$

Fig. 14. The optimum powertrain based on the weighted objective function, with tabulated vehicle specifications, corresponding scores, weighting factors, weighted scores and total weighted score.

design variable each time. These design variables are FC system power rating P_{FC}, battery power rating P_{batt}, battery energy capacity E_{batt}, electric machine module power rating P_{EM} and hydrogen storage capacity m_{H_2}. In this way, each plot shows a different distribution of the solutions according to the selected design variable and provides a visual sensitivity analysis of the weighted score against that design variable. The x-shaped data points scattered in diagrams represent the solutions (FCVs), while two maximum score curves, one for Topology C and one for Topology D, are created by simply connecting the FCVs with the highest scores. Looking at the range of the vertical axes, it is possible to see how the weighted score varies in the considered solution space.

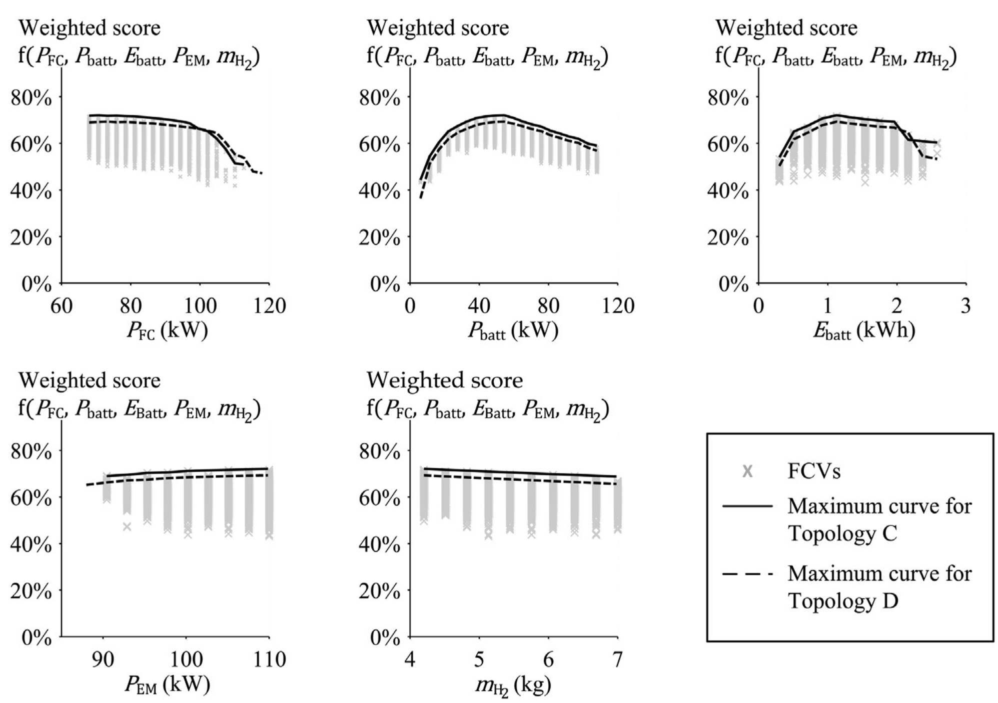

Fig. 15. Scatter plot based sensitivity analysis. Weighted score is shown as a function of five design variables, namely FC system power rating, battery power rating, battery energy capacity, electric machine module power rating and hydrogen storage capacity.

The maximum curves for Topology C and Topology D show that there is not a significant loss in design, when a topology choice needs to be made. The difference between these curves are so small and the forms are so similar that it is not possible to talk about a considerable advantage of a bi-port DC/DC converter against a three-port DC/DC converter. However, the FCV with the maximum weighted score is based on Topology C. This means that the assumed 10% improvement in costs, weight and volume of the constant high voltage components in Topology D is not enough for a better result. A further analysis shows that it needs to be assumed at least 20% improvement, so that higher scores with a three-port DC/DC converter are obtained.

The form of maximum score curves in the first diagram with FC system power rating in horizontal axis indicates that over-dimensioning the FC system until approx. 100 kW power rating does not cause any significant disadvantage. This range can also be called as reasonable design range for the FC system. However, after a certain power value there is a significant drop in weighted scores and it becomes impossible to design an FCV with a high score, no matter how other components are sized. The reasons for this behavior can be counted as, increasing costs, volume, weight; decrease in FC system efficiency and excessive power supply.

Unlike the FC system power rating, battery power rating reaches the maximum score around the middle of its design range. This shows that an optimum FCV powertrain design requires a certain minimum power output ability, which is necessary for hybrid functions. But on the other hand, it is also important not to over-dimension the battery, so that there is no excess power supply in the system. Similar to the battery power rating, battery energy capacity has also an optimum approximately in the middle of its design range, around 1.1 kWh. This behavior can also similarly be explained with the necessary minimum energy capacity for the hybrid functions and the disadvantageous extra weight, cost and volume that comes with extra energy capacity.

A relatively simple linear trend in maximum weighted score can be seen in the fourth diagram showing the electric machine module power rating. This can also be commented as a lower sensitivity of the weighted score against this design variable. Although the difference of the maximum weighted score through the design range is low, maximizing the electric machine power rating is advantageous. This can be explained with relatively low specific weight, cost and volume of this component and resulting increase in driving performance.

Similar to the electric machine, the hydrogen storage capacity shows a simple linear trend in maximum weighted score. However, this time the minimum value in the design range has the maximum score. This can be concluded as the optimum powertrain design should include a hydrogen storage system that is capable of holding the exact amount of the fuel that is necessary for the minimum required driving range, and not more. The main reason for this behavior can be counted as the high specific costs for the storage system. In addition, there are reasons, like increasing powertrain weight and volume.

The optimum FCV powertrain design in Fig. 14 is selected based on the weighting factors, which are defined according to a questionnaire. Due to the subjectivity in this technique, it is useful and necessary to check how the result is affected by altering the weighting factors in a further sensitivity analysis. In order to limit the number of variations in this sensitivity analysis, it is planned to consider only four different extreme cases. These cases are built simply by assuming that only one objective cluster (see Fig. 13) is weighted as 1, while the rest with 0 at each time. By doing so, it is aimed to find out the optimum powertrain designs at each case, where only the economic efficiency, driving performance, comfort or environmental impact is considered.

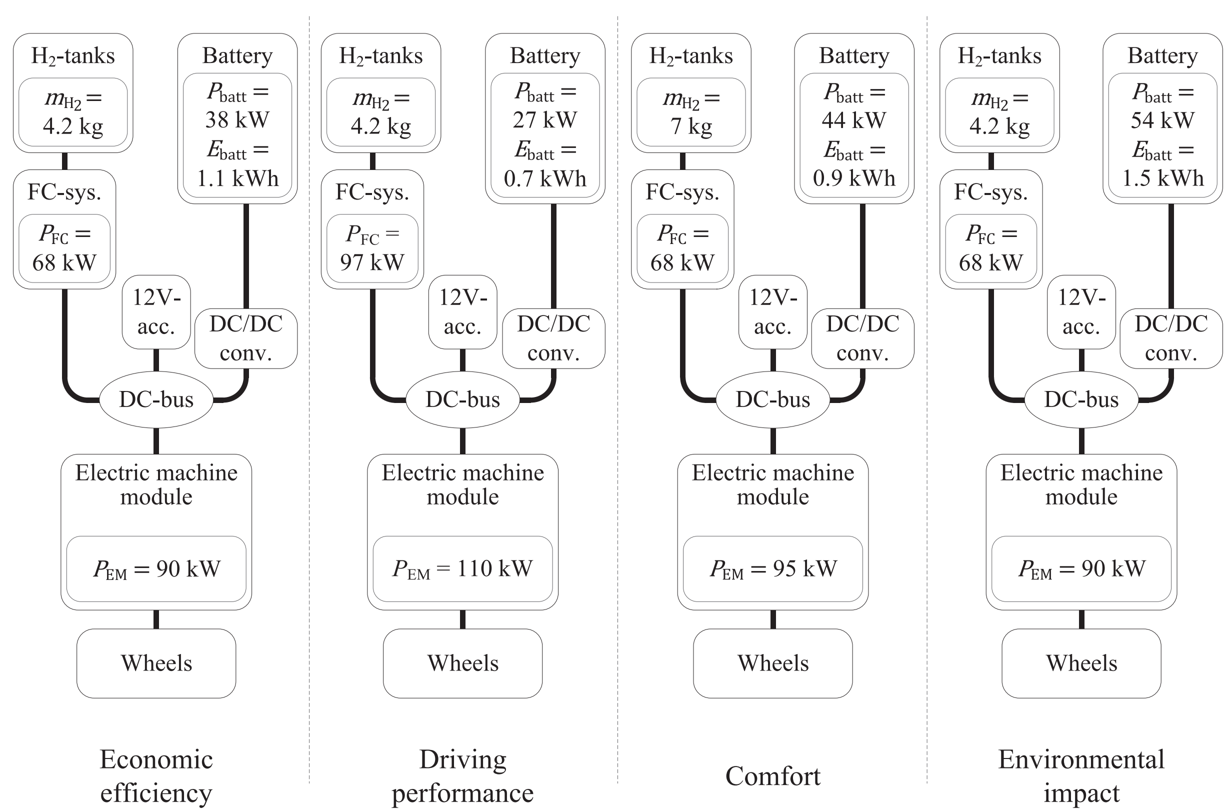

Fig. 16. The optimum FCV powertrains according to varying weighed objective functions, which are based on four different objective clusters.

Considering the results shown in Fig. 16 the optimum powertrain design differs in each case. The sizes of the components are varied, whereas the topology remains unchanged. In the first case, where the economic efficiency of the vehicle is considered, most of the components are smaller than the original optimum design (shown in Fig. 14) in order to lower the vehicle costs and reduce the fuel consumption. Secondly, the optimum powertrain design considering only driving performance objectives is shown. It is possible to see that the components, like battery and the hydrogen tanks are small in order to keep the powertrain weight low. On the other hand, the FC system and EM module power ratings are increased in order to supply a high continuous driving performance. The third optimum solution is selected based on the design objectives that are related to comfort. Desired maximum driving range causes that the hydrogen tanks' capacity is increased. On the other hand, the rest of the components are kept small in order to save volume and weight for the payload. Finally, the environmental impact is considered as a single design objective cluster. Since, in this case, the carbon dioxide emission is the single criterion and it is linearly proportional to hydrogen consumption, the solution with the lowest consumption is selected as optimum.

The selected four solutions and the original optimum solution differ in their powertrain designs, as well as in their vehicle specifications. In order to see how different certain vehicle specifications in these extreme cases are, these five solutions are plotted in Fig. 17 according to their vehicle cost scores (horizontal axis) and driving cost scores (vertical axis). Vehicle cost and driving cost are two important vehicle specifications that play a role in customer's decision. The scores are based on the other solutions in the non-dominated feasible solution space. Therefore, they provide a comparison-based consideration, which makes them more interesting than the absolute values of the properties in parentheses.

According to the distribution of the five FCVs, including four extreme cases, it is possible to identify the boundaries of a fair region on the vehicle cost vs. driving cost plot. It can be expected an optimum design of an FCV with different weighting factors will be around this region. The upper boundary of this region is defined by the most environment friendly FCV with 100% driving cost scores, whereas the lower boundary is defined by the sportier FCV at around 75%. The FCV with the highest economic efficiency is a good example for a low-cost vehicle and forms the right upper boundary of the region. However, buying more comfort can lower the vehicle cost and driving cost scores under 90%.

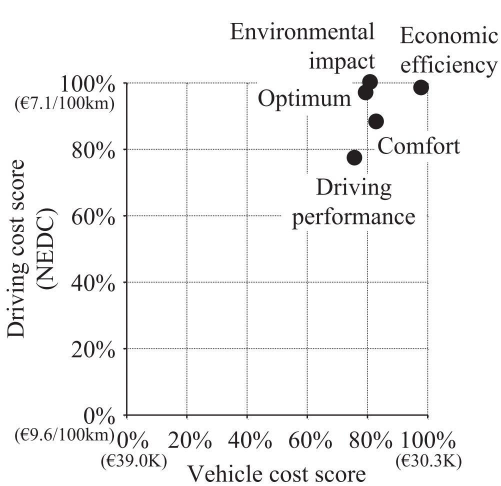

Fig. 17. Five FCVs, including four extreme cases of weighted objectives, on a vehicle cost score vs. driving cost score plot.

5. Conclusion

The proposed methodology is used in order to identify an optimum powertrain solution for a typical long-range FCV according to the given conditions, such as design requirements and objective weighting factors. Additionally, various trade-off and sensitivity analyses were demonstrated. In these demonstrations, not only qualitative conclusions are made, but also quantitative results are given. Indeed, one of the advantages of the proposed methodology is that it is possible to realize a comparative analysis within the non-dominated feasible solution space, since this group of solutions is completely known. Furthermore, it allows many possibilities in post processing without a need of a high computation power, such as possible changes in the objective function and reordering the solutions to reach a new one or realizing sensitivity analyses.

According to the results of this case study, the optimum FCV powertrain for a typical long-range vehicle is based on Topology C, which includes a DC/DC converter on the battery side. It has 4.2 kg hydrogen storage capacity, which is the lowest value for the required driving range. Its FC system delivers maximum 71 kW, which is slightly more than the continuous power requirement and provides a slightly better continuous driving performance than the minimum required. The 54 kW battery power rating, combined with 110 kW peak power rating of the electric machine, provides the necessary power rating for a high rate of regenerative braking and a high peak driving performance. On the other hand, its energy capacity of 1.1 kWh limits the peak driving performance duration, but it is enough for the desired duration and most of the hybrid functions to increase the vehicle efficiency.

References

[1] F. Küçükay, Grundlagen der Fahrzeugkonstruktion, Institut für Fahrzeugtechnik, Braunschweig, 2010. Lecture scripts.
[2] A. Elgowainy, A. Rousseaua, M. Wang, M. Ruth, D. Andress, J. Wardd, F. Joseck, T. Nguyend, S. Das, Energy Sustain. Dev. 17 (2013) 626–641.
[3] R. Edwards, J.-F. Larivé, J.-C. Beziat, Well-to-Wheels Analysis of Future Automotive Fuels and Powertrains in the European Context, European Comission Joint Research Centre Institute for Energy and Transport, Ispra, 2011.
[4] T. Katrašnik, Energy Convers. Manage. 50 (2009) 1924–1938.
[5] G. Rizzoni, L. Guzzella, B.M. Baumann, IEEE/ASME Trans. Mechatronics 4 (1999) 246–257.
[6] B.S.-M. Fan, Multidisciplinary Optimization of Hybrid Electric Vehicles: Component Sizing and Power Management Logic (PhD thesis), University of Waterloo, Waterloo, 2011.
[7] T. Hofman, D. Hoekstra, R.M.V. Druten, M. Steinbuch, in: IEEE Vehicle Power and Propulsion Conference in Chicago, 2005.
[8] B. Czapnik, Syntheses, Analyse und Bewertung von Antriebskonzepten (PhD thesis), Technischen Universität Carolo-Wilhelmina zu Braunschweig, Braunschweig, 2013.
[9] P. Rodatz, G. Paganelli, L. Sciarretta, Control Eng. Pract. 13 (2005) 41–53.
[10] I.L. Sarioglu, O.P. Klein, H. Schröder, F. Küçükay, IEEE Trans. Intell. Transp. 13 (2012) 1772–1781.
[11] A. Fadel, B. Zhou, J. Power Sources 196 (2011) 3271–3279.
[12] V. Paladini, T. Donateo, A.d. Risi, D. Laforgia, Energy Convers. Manage. 48 (2007) 3001–3008.
[13] D. Feroldi, M. Serra, J. Riera, IEEE Trans. Veh. Technol. 58 (2009) 4720–4729.
[14] M.-J. Kim, H. Peng, J. Power Sources 165 (2007) 819–832.
[15] J. Bernard, S. Delprat, F.N. Büchi, T.M. Guerra, IEEE Trans. Veh. Technol. 58 (2009) 3168–3176.
[16] L. Guzzella, A. Amstutz, IEEE Trans. Veh. Technol. 48 (1999) 1762–1769.
[17] M. Eghtessad, T. Meier, F. Küçükay, S. Rinderknecht, in: Hybrid and Electric Vehicles Symposium in Braunschweig, 2012.
[18] J.V. Mierlo, P.V.d. Bossche, G. Maggetto, J. Power Sources 128 (2004) 76–89.
[19] Hydrogenics, HyPM-HD Power Modules for Light and Heavy Duty Mobility. Available from: http://www.hydrogenics.com/docs/default-source/default-document-library/hypm-hd-power-modules.pdf?sfvrsn=0 (accessed 1.12.14).

[20] NuCellSys, Automotive HY-80 Fuel Cell System. Available from: http://www.nucellsys.com/dyn/mediaout.dhtml/2052d2da535d4c59887e/mime/PDF/HY-80-PDF/HY-80_2009.pdf (accessed 1.12.14).

[21] GM, Hydrogen Fuel Cell Propulsion System. Available from: http://www.hydrogen.energy.gov/pdfs/3_freese_0610.pdf (accessed 1.12.14).

[22] D.L. Greene, G. Duleep, Status and Prospects of the Global Automotive Fuel Cell Industry and Plans for Deployment of Fuel Cell Vehicles and Hydrogen Refueling Infrastructure, Oak Ridge National Laboratory, Oak Ridge, 2013.

[23] R.T. Doucette, M.D. McCulloch, J. Power Sources 196 (2011) 1163–1170.

[24] Cobasys, High Powered Hybrid Electric Vehicle Battery Systems Solutions. Available from: http://www.cobasys.com/pdf/transportation/NiMHax_HEV_Brochure.pdf (accessed 1.12.14).

[25] Wikipedia, Toyota Prius Plug-in Hybrid. Available from: http://en.wikipedia.org/wiki/Toyota_Prius_Plug-in_Hybrid (accessed 1.12.14).

[26] Wikipedia, Nissan Leaf. Available from: http://en.wikipedia.org/wiki/Nissan_Leaf (accessed 1.12.14).

[27] E.M. Krieger, C.B. Arnold, J. Power Sources 210 (2012) 286–291.

[28] R.K. Ahluwalia, T.Q. Hua, J.K. Peng, Int. J. Hydrogen Energy 37 (2012) 2891–2910.

[29] Strategic Analysis, Hydrogen Storage Cost Analysis, Preliminary Results. Available from: http://www.hydrogen.energy.gov/pdfs/review12/st100_james_2012_o.pdf (accessed 1.12.14).

[30] M. Olszewski, Evaluation of the 2010 Toyota Prius Hybrid Synergy Drive System, Oak Ridge National Laboratory, Oak Ridge, 2011.

[31] M.-H. Huh, D.Y. Park, J. Korean Stat. Soc. 37 (2008) 129–133.

[32] C. Bazgan, F. Jamain, D. Vanderpooten, Discrete Appl. Math. 161 (2013) 2841–2850.